14

Doppler Weather Radars and Wind Turbines

Lars Norin and Günther Haase
Swedish Meteorological and Hydrological Institute
Sweden

1. Introduction

In many countries the number of wind turbines is growing rapidly as a response to the increasing demand for renewable energy. The cumulative capacity of wind turbines worldwide has shown a near 10-fold increase in the last decade (Global Wind Energy Council, 2011) and in the coming years many more wind turbines are expected to be built. Existing, older wind turbines are likely to be replaced by larger, next generation, turbines.

Modern wind turbines are large structures, many reach more than 150 m above the ground. Clusters of densely spaced wind turbines, so called wind farms, are being built both on- and offshore.

The continued deployment of wind turbines and wind farms is, however, not unproblematic. Radar systems, for example, are easily disturbed by wind turbines. Interference caused by wind turbines is more severe for many radar systems than interference caused by, for example, masts or towers. This is due to the rotating blades of the wind turbines. Many Doppler radars use a filter that removes echoes originating from objects with no or little radial velocity. However, these filters do not work for moving objects such as the rotating blades of wind turbines. Wind turbines located in line of sight of Doppler radars can cause clutter, blockage, and erroneous velocity measurements, affecting the performance of both military- and civilian radar systems.

Even though both radars and wind turbines have been in use for many decades it is only in the last few years that the interference problem has received substantial attention. The reason for this is simple; in recent years wind turbines have increased in number and size and at the same time radar systems have become increasingly sensitive.

In this chapter we present a brief review of some of the work made to investigate the impact of wind turbines on Doppler weather radars. Starting with a historical overview we outline the evolution of wind turbines and early studies about their impact on Doppler radars in general and Doppler weather radars in particular. Three major interference types for Doppler weather radars are identified: clutter, blockage, and erroneous velocity measurements. Observations, models, and mitigation concepts for all three interference types are discussed.

In particular, we present results from a study on average wind turbine clutter, based on long time series of data. We show that modelling wind turbine clutter using the radar cross section of a wind turbine can lead to erroneous results. We further argue that blockage due to wind turbines is difficult to analyse using operational reflectivity data. An alternative way

of studying blockage is discussed and results are presented. A simple blockage model is described and its results are shown to agree with observations. Finally, examples of erroneous wind measurements are shown and mitigation measures are discussed.

2. Background

2.1 Wind turbine development

Wind power technology dates back many centuries. In the 1st century A.D. Hero of Alexandria described a simple wind wheel that could power an altar organ (Woodcroft, 1851). It is, however, not clear whether this invention was ever constructed or put to use. The first documented description of windmills that were used to perform irrigation and grinding grain comes from the region of Sistan, Persia, in the 9th century (Shepard, 1990). By the 12th century windmills were in use in Europe and in the following centuries they became increasingly important for grinding grain and pumping water. It was only after the industrial revolution their importance receded (Manwell et al., 2009).

Near the end of the 19th century the first wind turbines, used for the production of electricity, were developed. James Blyth built a 10 m high, cloth-sailed wind turbine in Scotland in 1887 (Price, 2005) and Charles Brush constructed a 25 m high wind turbine in Cleveland, Ohio, in 1887–1888 (Anon., 1890). A few years later, in the 1890s, Poul la Cour constructed over 100 wind turbines to generate electricity in Denmark (Manwell et al., 2009). In the 1970s the rising oil prices generated a renewed interest in wind power which led to serial production of wind turbines.

The increasing demand for renewable energy sources in the 21st century led to a further upswing for wind power. The pursuit of ever more powerful wind turbines lead to an increase in rotor blade diameter. A large wind turbine in the early 1980s could have a rotor diameter of 15 m and produce 55 kW whereas a large wind turbine in 2011 could have a rotor diameter larger than 150 m and produce 7 MW. Figure 1 shows the rotor diameter and the corresponding power produced by large wind turbines introduced on the market during the period 1981–2011.

Since wind turbines not only have become increasingly powerful but also grown more numerous during the last decades the global cumulative installed capacity has increased exponentially (see Fig. 2). With the exception of year 2010 the global annual installed capacity has increased monotonically since at least 1996 (cf. Fig. 2).

2.2 Wind turbine impact on Doppler radars

Wind turbines in the path of electromagnetic transmissions may cause interference by scattering parts of the transmitted signal but also by modulating the transmission's frequency. Initial studies on wind turbine interference focused on television and radio transmissions and showed that wind turbines could indeed cause interference to the reception of such signals (see, e.g., Sengupta (1984); Sengupta & Senior (1979); Senior et al. (1977); Wright & Eng (1992)).

By the end of the 20th century and beginning of the 21st century a large number of wind turbines had been installed and several investigations were conducted to analyse the impact of wind turbines on military surveillance radars and civilian air traffic control radars (see, e.g.,

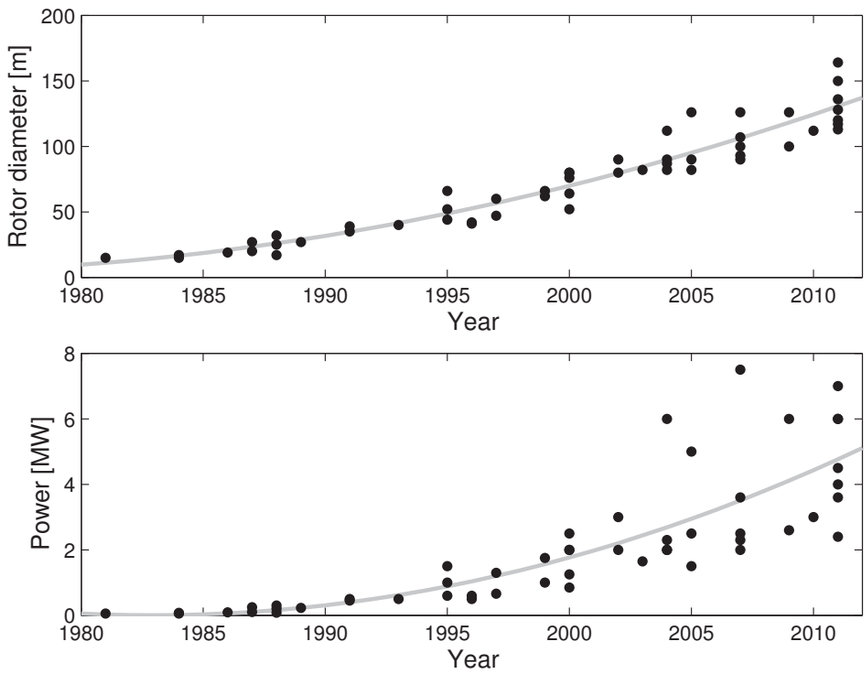

Fig. 1. Rotor diameter (top) and power (bottom) for a selection of large wind turbines introduced on the market during the period 1981–2011. Gray lines show superimposed trends. Data from The Wind Power (www.thewindpower.net) and wind turbine manufacturers' homepages.

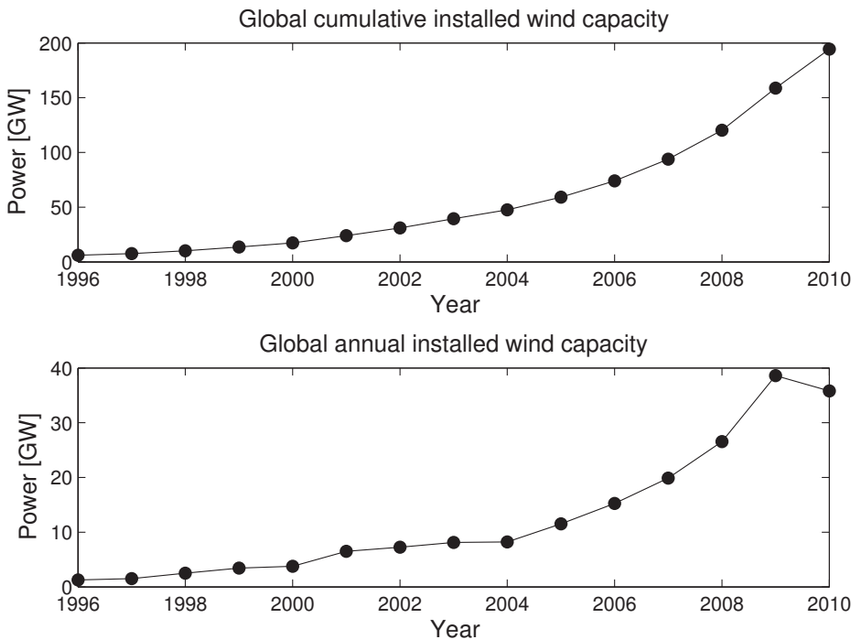

Fig. 2. Global cumulative installed wind capacity (top) and global annual installed wind capacity (bottom). Data from Global Wind Energy Council (2011).

Borely (2010); Butler & Johnson (2003); Davies (1995); Department of Defense (2006); Frye et al. (2009); Jago & Taylor (2002); Lemmon et al. (2008); Ousbäck (1999); Poupart (2003); RABC & CanWEA (2007); Sparven Consulting (2001); Summers (2001); Webster (2005a;b)). From these and other studies it became clear that wind turbines in general cause three types of problems for Doppler radars: clutter, blockage, and erroneous Doppler measurements.

- Clutter consist per definition of unwanted radar echoes. For a military surveillance radar clutter can for example consist of precipitation echoes whereas for a weather radar echoes from, e.g., aircraft are unwanted. Echoes from wind turbines are considered clutter by most radars.
- Blockage occurs when obstacles such as buildings or terrain obscure the radar line of sight. Measurements behind such obstacles become incomplete or non-existing. Wind turbines located near a radar may block a substantial part of the radar's measurement region.
- Doppler radars not only measure the echo strength of their targets but also their radial velocities. The motion of the rotor blades of a wind turbine is detected by the radar and may be interpreted as a moving target.

Clutter originating from the ground or from stationary buildings is often filtered out by built-in clutter filters that remove echoes with zero or low radial velocities. Echoes from the tower of a wind turbine have zero velocity and can therefore easily be removed but the turbine's rotating blades can have very large and variable velocities, escaping the clutter filter. Echoes from rotating wind turbine blades may therefore, for example, be mistaken for aircraft by an air traffic control radar.

Weather radar problems related to wind turbines were recognised early by Hafner et al. (2004) and Agence National des Fréquences (2005). These works have since been followed by many studies (e.g. Brenner et al. (2008); Donaldson et al. (2008); Haase et al. (2010); Hutchinson & Miles (2008); Toth et al. (2011); Tristant (2006a;b); Vogt et al. (2011; 2007a; 2009)). The increased awareness of the problems wind turbines may cause weather radars led both the World Meteorological Organization (WMO) and the Network of European Meteorological Services (EUMETNET) to issue general guidelines for the deployment of wind turbines, based on the distance from the radar (OPERA, 2010; WMO, 2010). These guidelines are summarised in Table 1 and Table 2.

3. Wind turbine interference

In the sections below we examine the three identified problems wind turbines can cause to Doppler weather radars: clutter, blockage, and erroneous wind measurements.

3.1 Clutter

For a weather radar, clutter refers to all non-meteorological radar echoes. Typical examples of clutter include echoes from terrain, buildings, and clear-air targets (e.g. insects, birds, atmospheric turbulence). Clutter can further be divided into two categories: static and dynamic. Static clutter typically originates from terrain and buildings whereas dynamic clutter is caused by moving targets such as clear-air returns. Static clutter has zero or near-zero radial velocity and can be removed by a built-in clutter filter whereas dynamic

Range	Potential impact	Guideline
0–5 km	The wind turbine may completely or partially block the radar and can result in significant loss of data that can not be recovered.	Definite Impact Zone: Wind turbines should not be installed in this zone.
5–20 km	Multiple reflection and multi-path scattering can create false echoes and multiple elevations. Doppler velocity measurements may be compromised by rotating blades.	Moderate Impact Zone: Terrain effects will be a factor. Analysis and consultation is recommended. Re-orientation or re-siting of individual turbines may reduce or mitigate the impact.
20–45 km	Generally visible on the lowest elevation scan; ground-like echoes will be observed in reflectivity; Doppler velocities may be compromised by rotating blades.	Low Impact Zone: Notification is recommended.
$>$ 45 km	Generally not observed in the data but can be visible due to propagation conditions.	Intermittent Impact Zone: Notification is recommended.

Table 1. WMO guidance statement on weather radar/wind turbine siting. (From WMO (2010))

Range	Radar	Statement
0–5 km	C-band	No wind turbine should be deployed within this range
5–20 km	C-band	Wind farm projects should be submitted for an impact study
0–10 km	S-band	No wind turbine should be deployed within this range
10–30 km	S-band	Wind farm projects should be submitted for an impact study

Table 2. Statement of the OPERA group on the cohabitation between weather radars and wind turbines. (From OPERA (2010))

clutter originates from targets having radial velocities larger than the clutter filter limits. Dynamic clutter can therefore not be suppressed by conventional clutter filters.

Operating wind turbines generate both static and dynamic clutter. Since the static clutter from the wind turbines is suppressed by clutter filters the dynamic wind turbine clutter, mainly originating from the rotating blades, has the largest impact on weather radar measurements. Dynamic wind turbine clutter (in the following referred to as wind turbine clutter) is often difficult to separate from precipitation echoes and may therefore incorrectly be interpreted by the weather radar as precipitation.

In addition, wind turbine clutter is highly variable in time since the amplitude of the scattered signal depends sensitively on the wind turbine's yaw- and tilt angle.

3.1.1 Observations

Observations of wind turbine clutter have been presented in numerous works (e.g. Agence National des Fréquences (2005); Burgess et al. (2008); Gallardo et al. (2008); Haase et al. (2010); Isom et al. (2009); Toth et al. (2011); Tristant (2006a); Vogt et al. (2011; 2007a)). The strength

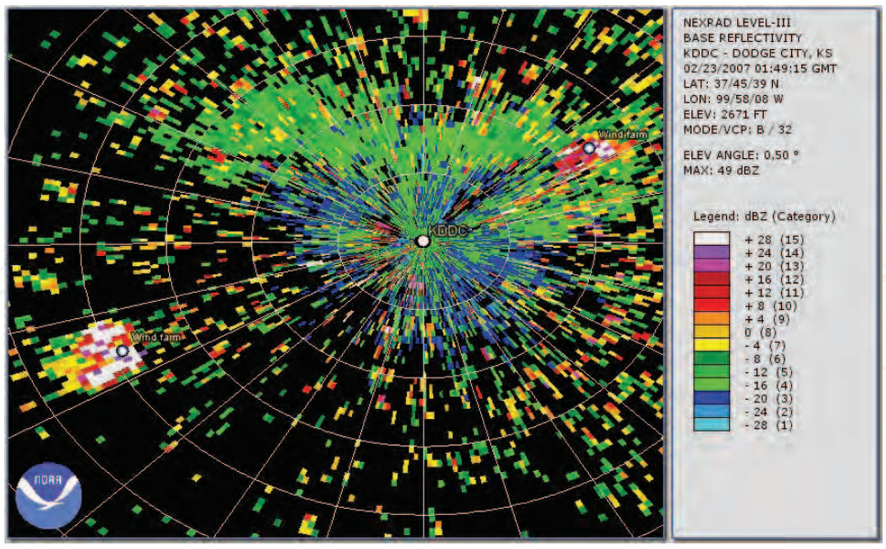

Fig. 3. Wind turbine clutter caused by two wind farms near Dodge City, Kansas, at 0149 GMT on February 23, 2007. One wind farm is located approximately 40 km to the southwest of the radar; the other near 20 km to the northeast. Range rings in white are at 10-km spacing. Adapted from Crum et al. (2008). This image was obtained from NOAA/National Climatic Data Center.

of the observed clutter can range from barely visible (< 0 dBZ) to near saturation levels ($>$ 60 dBZ) (Agence National des Fréquences, 2005; Crum et al., 2008; Toth et al., 2011; Tristant, 2006a).

An example of clutter, originating from two wind farms near Dodge City, Kansas, is shown in Fig. 3. One wind farm consists of 170 wind turbines and is located approximately 40 km southwest of the radar; the other wind farm consists of 72 wind turbines, located approximately 20 km northeast of the radar. On this otherwise clear day reflectivity values close to 30 dBZ can be seen at the location of both wind farms.

Images such as Fig. 3 convincingly demonstrate that wind turbine clutter exists and that it may indeed cause problems for weather radars. However, in order to obtain a quantitative estimate of wind turbine clutter long time series of data should be studied.

In the remainder of this section we present results from a study based on long time series of wind turbine clutter. In the study operational reflectivity data from the four lowest scans of all Swedish weather radars were analysed over a period of more than three years (November 1, 2007 to March 31, 2011). In order to estimate the amount of wind turbine clutter observed by the weather radars, precipitation echoes were filtered out using a custom-designed weather filter. To further increase the quality of the wind turbine clutter, all other clutter — here referred to as background clutter — was removed from the weather-filtered reflectivity data. Finally the wind turbine clutter (z) was converted to rain rate (R) assuming the relation $z = 200R^{1.5}$ (Michelson et al., 2000).

The weather filter removed precipitation echoes from the lowest elevation angle by comparing reflectivity data cellwise to reflectivities from a higher elevation angle. If an echo from a higher

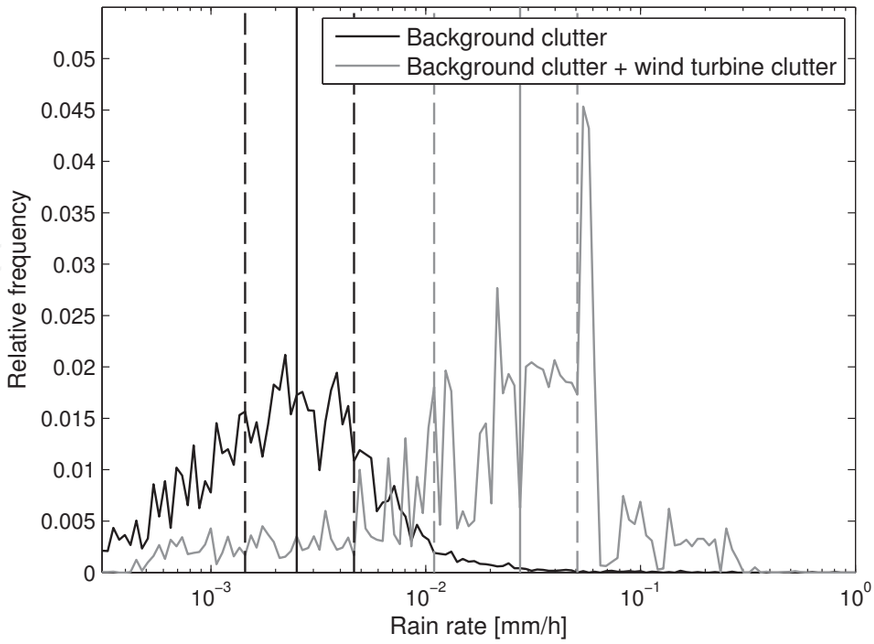

Fig. 4. Distributions of clutter before and after the construction of wind turbines. Solid, vertical lines indicate the median value and dashed, vertical lines show the first and third quartiles.

elevation angle was strong enough to indicate the presence of precipitation the corresponding value from the lowest elevation angle was filtered out.

Approximately 13 km from the weather radar in Karlskrona, Sweden, three wind turbines are located in the same radar cell (i.e., the same range bin and azimuth gate). Weather-filtered clutter distributions from this radar cell before and after the construction of the three wind turbines are shown in Fig. 4. It is seen that the two clutter distributions are easily distinguishable, having similar shapes but very different medians. It is evident that in this radar cell the existence of operational wind turbines has substantially increased the total amount of clutter.

Before the construction of the wind turbines, the reflectivity values remaining after filtering out precipitation echoes were composed of clear-air returns and other, non-identified, moving targets. In a second step of the analysis, this background clutter was removed from the weather-filtered reflectivity values recorded after the construction of the wind turbines. In this way a measure of clutter solely due to wind turbines was obtained.

The median wind turbine clutter was obtained from the difference between clutter after and before the construction of wind turbines. This analysis was carried out for all wind turbines in line-of-sight of a Swedish weather radar. The median wind turbine clutter values of 11 different radar cells, together with the first and third quartiles, are shown in Fig. 5. The median wind turbine clutter is seen to vary from close to zero to more than 0.02 mm h^{-1}. The spread of the clutter is attributed to the fact that the strength of a wind turbine echo depends on the position of the rotor blades and the yaw of the wind turbine, which in turn depends on the direction of the wind.

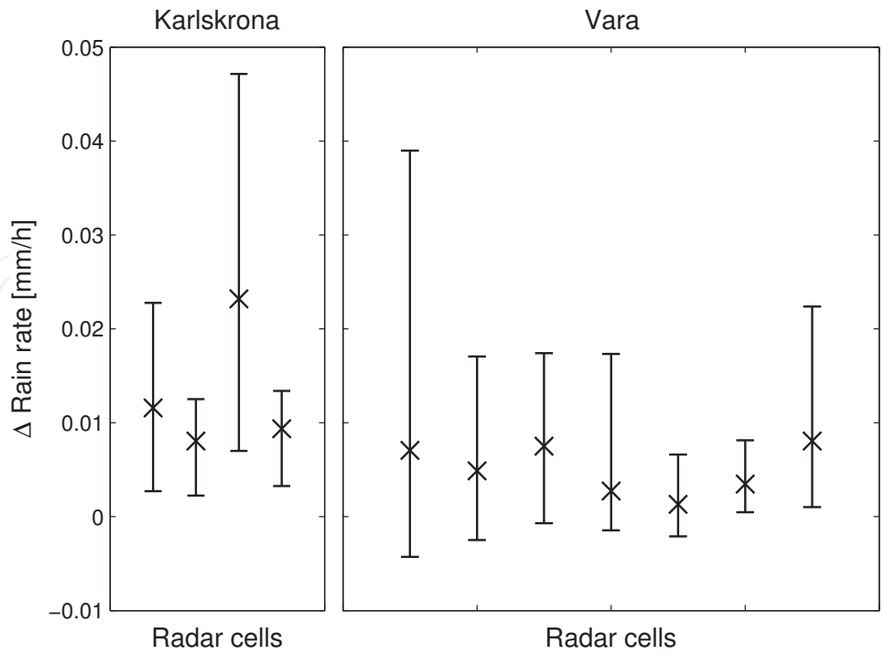

Fig. 5. Median wind turbine clutter together with first and third quartiles observed by two Swedish weather radars (Karlskrona and Vara).

Wind turbine clutter has also been observed from radar cells in which no wind turbines are located. An example of such area effects of wind turbine clutter is shown in Fig. 6. The wind turbine clutter in this figure comes from the same wind farm as in Fig. 4. All together this wind farm consists of five wind turbines with total heights of 150 m above the ground. Three of the five wind turbines are located within the same radar cell, the other two turbines each occupy a different radar cell. In Fig. 6 it is seen that not only the radar cells in which the wind turbines are located show an increase in clutter but also that several radar cells cross- and downrange of the turbines are affected.

Wind turbine clutter downrange from wind turbines (cf. Figs. 6a and b) has been observed in several other works (e.g. Crum et al. (2008); Haase et al. (2010); Isom et al. (2009); Toth et al. (2011); Vogt et al. (2011)). Such clutter tails can be visible for tens of kilometres behind wind turbines. No theoretical model has been put forward to explain this phenomenon but it has been suggested that the tails are caused by multiple scattering effects (scattering between multiple turbines and/or scattering between turbine and ground) (Crum et al., 2008; Isom et al., 2009; Toth et al., 2011). Clutter tails are not considered a problem for wind farms located further than 18 km from the weather radar (Crum & Ciardi, 2010; Vogt et al., 2009).

Cross-range clutter may also occur, as is seen in Figs. 6a and c. For the case shown in Fig. 6, the cross-range clutter is a direct result of the way the reflectivities are stored in the radar data matrix (the azimuthal resolution of the actual radar measurements is lower than the azimuthal spacing of the data matrix). However, for wind turbines generating very strong echoes it has been suggested that clutter may be seen well outside the half-power width of the radar beam, generating cross-range clutter spanning tens of degrees (Agence National des Fréquences, 2005).

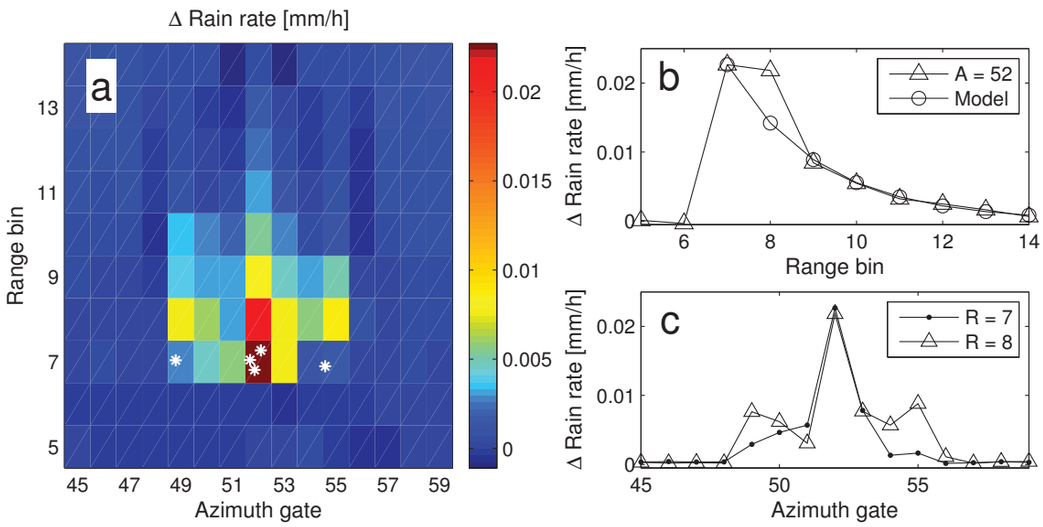

Fig. 6. Wind turbine clutter caused by a wind farm approximately 13 km northeast of the Karlskrona weather radar. a) Clutter from an area containing five wind turbines (shown by white asterisks). One wind turbine is located in radar cell [7,49], three are located in [7,52], and one in [7,55]. b) Clutter from azimuth gate 52 together with model results. c) Clutter from range bins 7 and 8.

3.1.2 Models

Most models of wind turbine clutter rely on the turbines' radar cross section (RCS) as a measure of how efficiently radar pulses are backscattered (Agence National des Fréquences, 2005; Tristant, 2006a). In order to model wind turbine clutter the RCS of a wind turbine must be converted to the equivalent radar reflectivity factor. The radar equation for point targets is given by (see, e.g. Skolnik (2008))

$$P_r = \frac{P_t G^2 \lambda^2 \sigma}{64\pi^3 D^4} \tag{1}$$

where P_r and P_t are, respectively, the power received and transmitted by the radar, G is the antenna gain, λ is the wavelength, σ is the RCS of the target, and D is the distance from the radar to the target.

For distributed targets, such as rain, the radar equation is written as (see, e.g. Keeler & Serafin (2008))

$$P_r = \frac{P_t G^2 \theta \phi c \tau \pi^3 |K|^2 z}{1024 \ln(2) \lambda^2 D^2} \tag{2}$$

where θ and ϕ are the azimuth and elevation beamwidths, c is the speed of light, τ is the radar pulse width, $|K|^2$ is a parameter related to the complex index of refraction of the material, and z is the linear radar reflectivity factor. For a given RCS the linear radar reflectivity factor can thus be expressed as

$$z = C_1 \frac{\sigma}{D^2} \tag{3}$$

where C_1 is a constant that depends on the parameters of the radar system. For Swedish weather radars, $C_1 = 3 \times 10^{12}$ mm^{6}m^{-3}.

Let us use Eq. (3) to calculate what RCS would cause an observed rain rate of $R = 0.1$ mm h^{-1} (cf. Fig. 4) at a distance $D = 13$ km from the radar. Using $z = 200R^{1.5}$ we find that $\sigma = 4$ cm^2.

The RCS of wind turbines has been studied both experimentally and numerically (see, e.g., Greving & Malkomes (2006); Kent et al. (2008); Kong et al. (2011); Ohs et al. (2010); Poupart (2003); Zhang et al. (2011)). These studies have shown that RCSs of wind turbines display a sensitive dependence on yaw- and tilt angle. However, measurements of the RCS of large wind turbines typically range between 20 to 30 dBsm (Kent et al., 2008; Poupart, 2003) which is very far from what we obtained in the calculation. Using the RCS to calculate wind turbine clutter in this simple way may therefore lead to erroneous results.

It has been argued that the RCS is not applicable to wind turbines (Greving & Biermann, 2008; Greving et al., 2009; Greving & Malkomes, 2006; 2008). The reason is that the plane wave condition does not hold for objects on the ground. From the calculation above it is clear that more sophisticated models are needed in order to make a correct simulation of wind turbine clutter.

For downrange clutter a simple, empirical model was constructed using an exponential function to fit the limited amount of data available. The rain rate R behind a wind turbine was modelled as

$$R = R_0 \exp\left(-\frac{C_2 x}{N}\right) \tag{4}$$

where R_0 is the rain rate in mm h^{-1} from the radar cell containing the wind turbine, $C_2 = 0.7$ is an empirically determined constant, x is the distance behind the wind turbine in kilometres, and N is the number of interfering wind turbines present in the radar cell. Observations and model results are shown in Fig. 6b.

3.1.3 Mitigation concepts

Various concepts for mitigating wind turbine clutter have been suggested in different studies. Some of these concepts are listed here.

- Placing wind turbines so that they are not in line of sight of a weather radar. Under normal conditions a radar's measurements will not be affected by objects that are not in the radar line of sight. This method is therefore a certain way of limiting wind turbine clutter. It has also been suggested that wind turbines should be arranged radially from the radar. Such a formation probably does little to mitigate clutter since the blades of the different wind turbines do not move synchronously.
- Reducing the wind turbines' RCS. It has been proposed that stealth materials can be applied to wind turbines as a way of reducing the RCS (Appelton, 2005; Butler & Johnson, 2003). Studies of stealth coating wind turbine blades show that a reduction of more than 10 dB may be possible (Rashid & Brown, 2010), making it an interesting solution. An alternative way of reducing the rotor blades' RCS is to modify their shape, but this is not considered a realistic alternative as the shape of a rotor blade is optimized for efficiency.
- Adaptive clutter filters. Various filter techniques for removing or reducing effects of wind turbine clutter have been suggested. Gallardo et al. (2008) suggested using an image processing technique and Isom et al. (2009) proposed a multiquadratic interpolation technique. Other signal processing techniques have also been proposed (Bachmann et al.,

2010a;b; Gallardo-Hernando & Pérez-Martínez, 2009; Nai et al., 2011). These methods all use raw data as input, i.e., in- and quadrature phase (I/Q) data.

To speed up filtering, only radar cells containing wind turbines should ideally be processed. This may be achieved by keeping maps of all wind turbines near a weather radar or by using automatic detection schemes (Cheong et al., 2011; Gallardo-Hernando et al., 2010; Hood et al., 2009; 2010).

- Gap-filling radars. Areas contaminated by clutter may be covered by a second, nearby radar, a so-called gap-filler (Aarholt & Jackson, 2010; Department of Defense, 2006; Ohs et al., 2010). This alternative may be a convenient solution for specific cases but could also lead to even bigger problems since an introduction of additional radars introduces new sites which also must be protected.
- Adaptation of the radar scan strategy. Changing the radar scan strategy to pass over areas with wind turbines will limit the amount of clutter received. The drawback is that data will be gathered from higher altitudes which may shorten the effective range of the radar.

3.2 Blockage

For a weather radar, blockage manifests itself as a reduction of the expected precipitation echoes downrange from an obstacle. But, as we have seen in Section 3.1, obstacles in line of sight of a radar do not only cause blockage, they also cause clutter. Stationary obstacles cause static clutter which can be removed by a clutter filter. However, dynamic clutter, such as echoes from rotating blades of wind turbines, is not removed by the clutter filter. Downrange from such obstacles both clutter and blockage can appear. For wind turbines in line of sight of a weather radar the increased echo strength from the clutter can often be as large, or larger, than the reduction in echo strength due to blockage. Separating the effects of blockage and clutter is therefore often impossible using data analysis. However, large wind farms may cause substantial blockage and the effect may be visible for tens of kilometres downrange of the farm.

3.2.1 Observations

Blockage caused by wind turbines is not always visible in radar reflectivity images. As explained previously this is partly due to clutter tails but also because precipitation echoes are not always spatially homogeneous.

One example of blockage caused by a wind farm near Dodge City, Kansas, is shown in Fig. 7. In the figure a weak shadow can be seen behind a wind farm to the southwest of the weather radar. Other examples of blockage caused by wind turbines can be found in Vogt et al. (2007a) and Seltmann & Lang (2009).

As mentioned above, making a quantitative analysis of blockage behind wind farms is difficult due to clutter tails and the spatial variation of precipitation echoes. Let us therefore instead examine blockage caused by a stationary structure in line of sight of a weather radar.

The air traffic control tower of Arlanda Airport near Stockholm, Sweden, is located only 0.9 km from the Arlanda weather radar. The full width at half maximum of the radar beam is 0.9°, which at the distance of the tower corresponds to approximately 14 m. The radar beam is

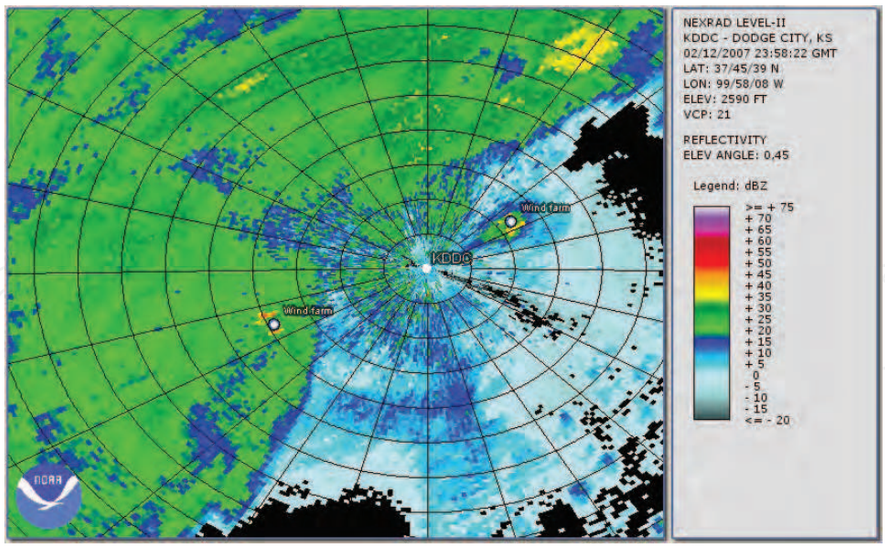

Fig. 7. Reflectivity measurement from the weather radar near Dodge City, Kansas, at 2358 GMT, February 12, 2007. Blockage caused by a wind farm to the southwest results in a reduction of precipitation echoes downrange from the wind farm (most clearly visible at a distance of 70–100 km from the radar). Range rings in black are at 10-km spacing. Adapted from Burgess et al. (2008). This image was obtained from NOAA/National Climatic Data Center.

thus wider than the width of the tower (approximately 8.5 m). For the lowest elevation angle of the radar the tower fills the entire beam height.

The average amount of precipitation per hour, for the period 1 November 2007 to 31 March 2011, is shown in Fig. 8. In this figure it is seen that some azimuth gates have considerably less measured precipitation compared to their neighbours. These gates coincide with the location of the tower.

One way to obtain a quantitative estimate of the reduction in expected precipitation due to blockage is to assume that the precipitation can be considered constant over some neighbouring azimuth gates. To validate this assumption a correlation analysis was performed. The analysis revealed that the correlation between precipitation measurements from neighbouring azimuthal radar cells depends on cross-range distance and accumulation period. The correlation decreases as the cross-range distance increases and for the same cross-range distance, shorter accumulation periods results in lower correlation. Applying the correlation analysis to the precipitation measured by the Arlanda weather radar showed that, for example, precipitation from radar cells with cross-range distances up to 5 km and an accumulation period of 24 h had a correlation over 0.9.

To obtain a measure of how much precipitation varies locally the coefficient of variation of accumulated precipitation from neighbouring azimuthal radar cells was calculated. In the analysis for the Arlanda weather radar it was shown that the coefficient of variation increased with increasing number of neighbouring azimuthal gates (i.e. window size) and decreased with accumulation period.

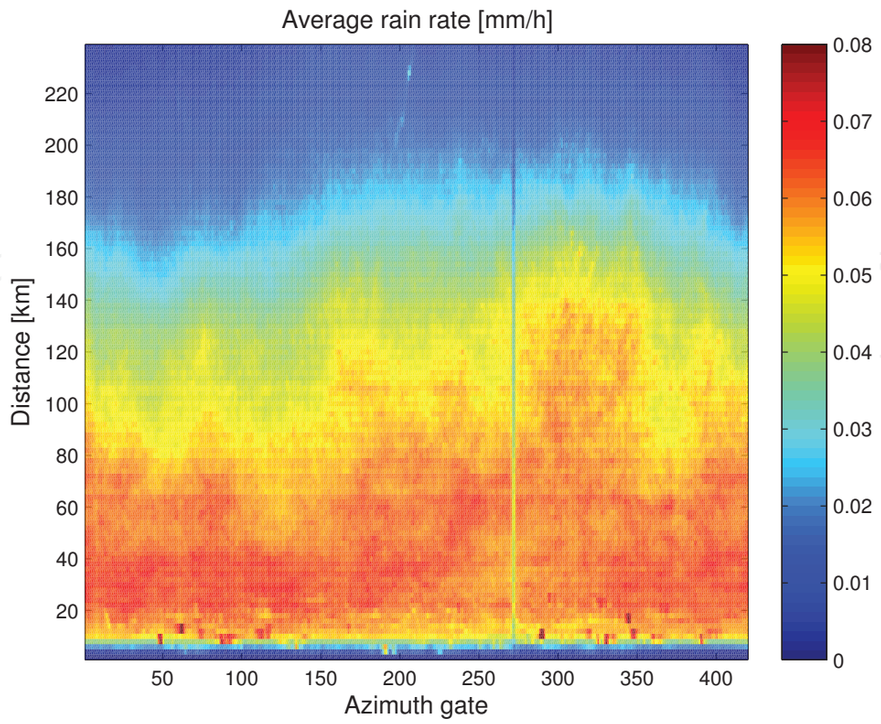

Fig. 8. Average amount of precipitation per hour from the lowest elevation angle (0.5°) for the weather radar at Arlanda airport, Sweden. Blockage caused by a nearby air traffic control tower can be seen near azimuth gate 271.

For example, for an accumulation period of 1 hour and a window size of 13 gates (corresponding to 11.7° in azimuthal angle) the coefficient of variation did not decrease lower than approximately 0.25 at any distance from the radar whereas for an accumulation period of 1 month the coefficient of variation for the same number of gates was lower than 0.05 at 10 km from the radar. The coefficient of variation can be compared with the blockage caused by an obstacle.

To find a quantitative estimate of the reduction in expected precipitation echoes caused by the Arlanda tower a 13-gate wide window was applied to the data, accumulated over the entire three-year-period. The measurements in the window were normalized over azimuth and range to the average value of unaffected gates. In Fig. 9 it is seen that the measured precipitation is reduced by close to 30% in the most severely affected gate.

Comparing the blockage of the Arlanda tower with the coefficient of variation for various accumulation periods it was found that on average between 24 hours and 1 week was needed for the coefficient of variation of the local precipitation to be lower than 30%. On individual radar images it may therefore be difficult to see the effects of the Arlanda tower blockage.

3.2.2 Models

Modelling of electromagnetic shadow effects can be done with varying accuracy and complexity. Methods and results of modelling blockage and shadow effects downrange of wind turbines can be found in, e.g., Belmonte & Fabregas (2010); Greving & Malkomes

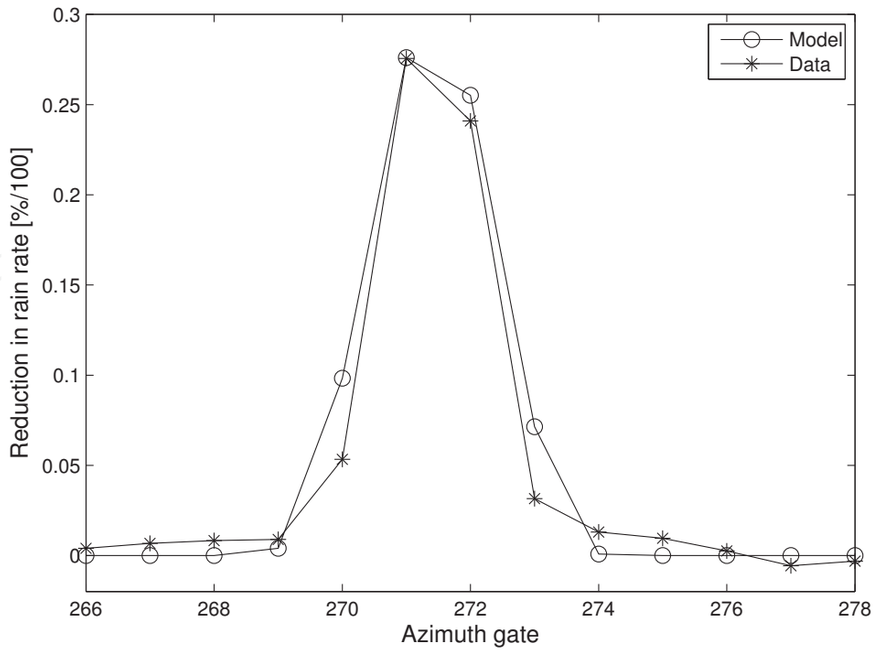

Fig. 9. Blockage caused by an air-traffic control tower at Arlanda Airport. Data and model.

(2008); Høye (2007). Here we describe a simple and computationally light method to calculate blockage caused by an obstacle.

As a first approximation of the reduction in returned power due to an obstacle we consider the obstacle's geometrical cross section. Convolving the obstacle's cross section with the radar beam's power flux and dividing by the total power from an unperturbed beam we obtain the fraction of power, P_{B}, blocked by the obstacle. To find the corresponding reduction in rain rate we start by noting that $1 - P_{\mathrm{B}}$ is the amount of power that is unaffected by blockage. The (unaffected) power is proportional to the linear radar reflectivity factor z according to Eq. (2) and z is in turn related to rain rate R by $z \propto R^{1.5}$. Hence the reduction in rain rate, R_{B}, can be expressed as $R_{\mathrm{B}} = 1 - (1 - P_{\mathrm{B}})^{1/1.5}$.

Applying this method to the Arlanda air-traffic control tower described in Section 3.2.1 we can estimate the reduction in rain rate it causes. The modelled reduction in rain rate is shown in Fig. 9 together with the observations. The model is seen to capture the magnitude and the cross-range shape of the blockage. This model can be used for estimating blockage caused by wind turbines, but for reasons explained in Section 3.2.1 there are no observations to compare these results with.

3.2.3 Mitigation concepts

Methods proposed to prevent or reduce blockage by wind turbines include:

- Optimising the placement of the wind turbines. Wind turbines should preferably be placed out of the line of sight of the radar. Otherwise it has been suggested that wind turbines should be arranged radially from the radar. In this way the blockage caused by the wind

turbine towers may be reduced, but blockage caused by rotor blades will persist since there is no synchronisation of their movements.

- Use of a gap-filling radar. A way to remove or reduce blockage is to place an additional radar to cover areas affected by blockage.
- Adapting the radar scan strategy so that the radar beam passes over areas with wind turbines. This method ensures that measurements are not affected by blockage but in return data will be gathered from higher altitudes.

3.3 Wind measurements

A Doppler radar measures frequency shifts of the received signals and translates the shifted frequencies to radial velocities. A conventional clutter filter removes echoes with low or zero frequency shifts and thereby prevents static clutter from entering the radar products.

Signals scattered from rotating blades of a wind turbine are shifted in frequency and thereby interpreted by the radar as moving objects, escaping the clutter filter. The tip of a rotor blade can move with a velocity up to 100 m s^{-1} whereas close to the hub the blade velocity is close to zero. The scattered signals will therefore display a broad distribution in frequency space. The wind velocity is normally estimated as the strongest (non-zero) frequency component. Since echoes from wind turbines often are stronger than weather echoes this can lead the weather radar to display erroneous wind measurements.

3.3.1 Observations

There are many observations of wind turbines causing erroneous wind measurements in the literature (see, e.g., Burgess et al. (2008); Cheong et al. (2011); Crum et al. (2008); Haase et al. (2010); Isom et al. (2009); Toth et al. (2011); Vogt et al. (2007a)). One such example from the weather radar in Dodge City, Kansas, is shown in Fig. 10. From this figure it is clear that at the time of the measurements the overall wind direction was to the northwest but signals from radar cells containing a large wind farm, approximately 40 km to the southwest, show up as having close to zero velocity. In Fig. 11 is shown the spectrum width of the velocity measurements and from this figure it is clear that there is a significant broadening of the frequency spectra over the wind farm.

These observations can be understood by examining the raw I/Q data from the radar. Spectrograms of I/Q data, containing echoes from wind turbines, show highly complex and richly structured patterns. Examples of such spectrograms are given by, e.g., Bachmann et al. (2010a); Gallardo et al. (2008); Gallardo-Hernando & Pérez-Martínez (2009); Gallardo-Hernando et al. (2009); Hood et al. (2009); Isom et al. (2009); Nai et al. (2011); Poupart (2003); Vogt et al. (2007a;b). From these and other studies it is clear that echoes from wind turbine rotor blades in different positions result in broad distributions in frequency space even though the average velocity estimate is often close to zero.

As for wind turbine clutter there are observations showing tails of erroneous wind measurements behind the wind turbines (Burgess et al., 2008; Seltmann & Lang, 2009; Vogt et al., 2007a; 2009).

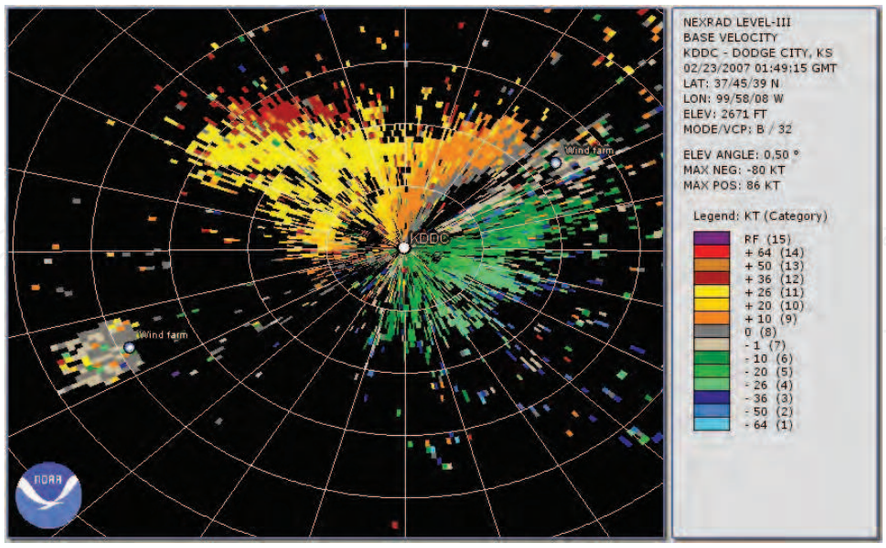

Fig. 10. Wind measurements from the weather radar near Dodge City, Kansas, at 0149 GMT, on February 23, 2007. The general wind direction is to the northwest but measurements near a wind farm to the southwest of the radar show wind velocities close to zero. Range rings in white are at 10-km spacing. Adapted from Vogt et al. (2007a). This image was obtained from NOAA/National Climatic Data Center.

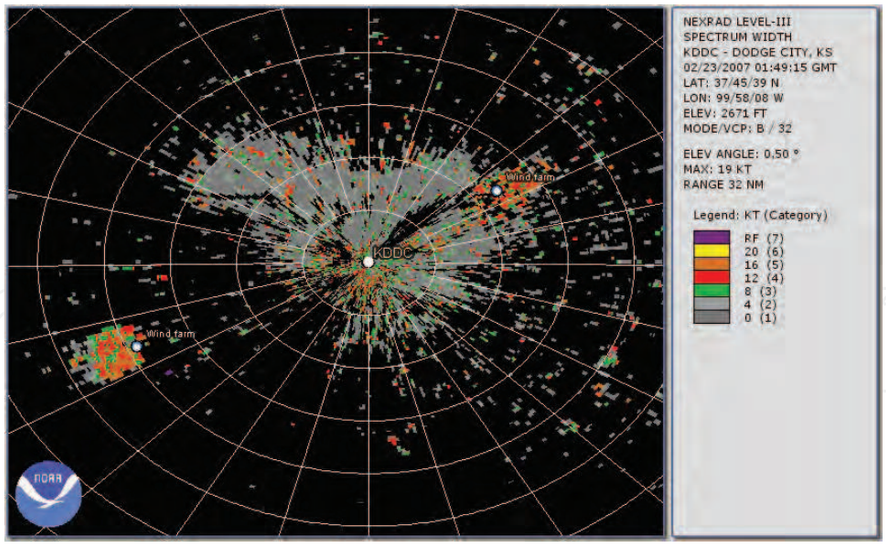

Fig. 11. Measurements of spectrum width from the weather radar near Dodge City, Kansas, at 0149 GMT, on February 23, 2007,. The spectrum widths are considerably enhanced near a wind farm to the southwest of the radar. Range rings in white are at 10-km spacing. Adapted from Vogt et al. (2007a). This image was obtained from NOAA/National Climatic Data Center.

3.3.2 Models

A few methods have been proposed to model the frequency spectra generated by wind turbines (Gallardo-Hernando et al., 2010; Hood et al., 2009; 2010; Kong et al., 2011; Zhang et al., 2011). In these models clutter from the tower, hub, and rotor blades are included. The model results show the zero-velocity returns of the tower, near-zero returns of the hub, as well as spectral broadening of the blades.

3.3.3 Mitigation concepts

Most concepts proposed to prevent or reduce clutter (see Section 3.1.3) are also valid for erroneous wind measurements.

Adaptive filters, suggested for removing wind turbine clutter, can also help mitigate erroneous wind measurements. If clutter is removed from the signal, the average wind velocity as well as the spectrum width can easily be estimated. Suggestions for adaptive wind filters can be found in, e.g., Bachmann et al. (2010a;b); Gallardo et al. (2008); Isom et al. (2009); Nai et al. (2011). As for the adaptive clutter filters, all these methods use raw I/Q data as input.

4. Conclusions

In many countries the number of wind turbines is growing rapidly as a response to the increased demand for renewable energy. As wind turbines grow larger and more numerous potential conflicts with other interests are emerging. Doppler radars, for example, are easily disturbed by wind turbines. In this chapter we have presented an overview on wind turbine-related problems experienced by Doppler weather radars. Three main wind turbine-related problems have been identified: clutter, blockage, and erroneous wind measurements.

Clutter — unwanted radar echoes — are generated by all obstacles in line of sight of a radar. Static clutter, i.e., echoes with no or low radial velocities are easily removed by the Doppler radar's built-in clutter filter. However, the moving blades of a wind turbine generate dynamic clutter which displays a wide range of radial velocities that cannot be removed by a conventional clutter filter. In this chapter it has been shown that wind turbine clutter can be problematic for weather radars since such echoes are interpreted as precipitation. Wind turbine clutter can display a large variation in strength, ranging from barely visible to near saturation levels of the radar. Behind wind turbines a tail of clutter can often be seen. This phenomenon is believed to be the result of multiple scattering effects. In an example shown in this chapter, clutter tails were seen to decrease exponentially behind the wind turbines. Cross-range clutter has also been observed. This can be caused by differences in azimuthal resolution of the actual radar measurements and azimuthal spacing of the radar data matrix but it has also been suggested that it may occur as a result of the radar sidelobes.

The magnitude of wind turbine clutter is often estimated by calculating the radar cross section of wind turbines. Such models may lead to results inconsistent with observations. Effects from the ground and terrain should be taken into account, otherwise a calibration of the model may be necessary.

Possible mitigation measures for wind turbine clutter include a) placing wind turbines out of the radar's line of sight b) reducing the wind turbines' radar cross section using stealth material c) development and application of adaptive clutter filters, d) use of gap-filling radars to cover areas contaminated by clutter and e) adapting the radar scan strategy to pass over the wind turbines.

Blockage is caused by any obstacle in line of sight of a radar and is not specific to wind turbines. For a weather radar, blockage leads to an underestimation of the precipitation behind the blocking obstacle. Blockage caused by wind turbines is difficult to analyse using reflectivity data due to spatial variation of precipitation and clutter tails that are generated behind wind turbines. Model results can, however, be compared with observations of blockage caused by stationary obstacles such as towers, masts, or wind turbines that are not in operation.

Concepts for mitigating blockage include a) placing wind turbines radially from the radar b) use of a gap-filling radar to cover affected areas and c) adapting the radar scan strategy to pass over the wind turbines.

The Doppler function of a radar detects movements in echoes such as those from the rotating blades of a wind turbine. Although such measurements are correct, the interpretation by the radar may still be wrong. For example, an air traffic control radar may interpret echoes from rotating wind turbine blades as a moving aircraft and a weather radar may interpret such measurements as an approaching thunderstorm.

A weather radar uses Doppler-shifted echoes to estimate the wind speed. Doppler-shifted echoes from wind turbine blades may therefore lead to erroneous wind measurements. Observations of wind measurements over wind farms occasionally show extremely large wind speeds but most often the wind measurements are close to zero. The non-synchronised movements of the many rotor blades of a wind farm also lead to large spectrum widths.

Mitigation measures for wind measurements are the same as those presented for wind turbine clutter.

5. References

Aarholt, E. & Jackson, C. A. (2010). Wind farm gapfiller concept solution, *European Radar Conference*, EuRAD, Paris, pp. 236–239.

Agence National des Fréquences (2005). Perturbations du fonctionnement des radars meteorologiques par les eoliennes, *Technical Report Rapport CCE5 No.1*, Commision Consultative de la Compatibilité Electromagnétique. In French.

Anon. (1890). Mr. Brush's windmill dynamo, *Scientific American* 63(25): 54.

Appelton, S. (2005). Design & manufacture of radar absorbing wind turbine blades, *Final Report W/44/00636/00/REP, DTI PUB URN 05/1409*, QinetiQ.

Bachmann, S., Al-Rashid, Y., Bronecke, P., Palmer, R. & Isom, B. (2010a). Suppression of the windfarm contribution from the atmospheric radar returns, *26th Conference on Interactive Information and Processing Systems for Meteorology, Oceanography, and Hydrology*, American Meteorological Society, pp. 81–86.

Bachmann, S., Al-Rashid, Y., Isom, B. & Palmer, R. (2010b). Radar and windfarms — mitigating negative effects through signal processing, *The Sixth European Conference on Radar in Meteorology and Hydrology*, ERAD, Sibiu, Romania, pp. 81–86.

Belmonte, A. & Fabregas, X. (2010). Analysis of wind turbines blockage on doppler weather radar beams, *IEEE Antennas and Wireless Propagation Letters* 9: 670–673.

Borely, M. (2010). Guidelines on how to assess the potential impact of wind turbines on surveillance sensors, *Technical Report EUROCONTROL-GUID-130*, EUROCONTROL.

Brenner, M., Cazares, S., Cornwall, M. J., Dyson, F., Eardley, D., Horowitz, P., Long, D., Sullivan, J., Vesecky, J. & Weinberger, P. J. (2008). Wind farms and radar, *Technical Report JSR-08-126*, JASON.

Burgess, D. W., Crum, T. D. & Vogt, R. J. (2008). Impacts of wind farms on WSR-88D radars, *24th International Conference on Interactive Information and Processing Systems for Meteorology, Oceanography, and Hydrology*, American Meteorological Society. Paper 6B.3.

Butler, M. M. & Johnson, D. A. (2003). Feasibility of mitigating the effects of windfarms on primary radar, *Department of Trade and Industry report ETSU W/14/00623/REP*, Alenia Marconi Systems Limited.

Cheong, B. L., Palmer, R. & Torres, S. (2011). Automatic wind turbine detection using level-II data, *2nd Conf. on Weather, Climate, and the New Energy Economy*, Amererican Meteorological Society, Seattle, WA. Paper 808.

Crum, T. & Ciardi, E. (2010). Wind farms and the WSR-88D: An update, *Nextrad Now* 20: 17–22.

Crum, T., Ciardi, E. & Sandifer, J. (2008). Wind farms: Coming soon to a WSR-88D near you, *Nextrad Now* 18: 1–7.

Davies, N. G. (1995). Wind farm radar study, *Technical Report ETSU-W–32/00228/49/REP*, Energy Technology Support Unit.

Department of Defense (2006). The effect of windmill farms on military readiness, *Report to the congressional defense committees*, Office of the Director of Defense Research and Engineering. [Available online at http://www.defense.gov/pubs/pdfs/windfarmreport.pdf].

Donaldson, N., Best, C. & Paterson, B. (2008). Development of wind turbine assessments for Canadian weather radars, *The Fifth European Conference on Radar in Meteorology and Hydrology*, ERAD, Helsinki, Finland.

Frye, A., Neumann, C. & Müller, A. (2009). The compatibility of wind turbines with radars, *Annual Report 54.7100.035.12*, European Aeronautic Defence and Space Company.

Gallardo, B., Pérez, F. & Aguado, F. (2008). Characterization approach of wind turbine clutter in the Spanish weather radar network, *The Fifth European Conference on Radar in Meteorology and Hydrology*, ERAD, Helsinki, Finland.

Gallardo-Hernando, B. & Pérez-Martínez, F. (2009). Wind turbine clutter, *in* G. Kouemou (ed.), *Radar Technology*, InTech, Croatia.

Gallardo-Hernando, B., Pérez-Martínez, F. & Aguado-Encabo, F. (2009). Mitigation of wind turbine clutter in C-band weather radars for different rainfall rates, *Proceedings of the 2009 International Radar Conference*, Bordeaux, France.

Gallardo-Hernando, B., Pérez-Martínez, F. & Aguado-Encabo, F. (2010). Wind turbine clutter detection in scanning weather radar tasks, *The Sixth European Conference on Radar in Meteorology and Hydrology*, ERAD, Sibiu, Romania.

Global Wind Energy Council (2011). Global wind report – annual market update 2010, *Technical report*, Global Wind Energy Council. [Available online at: http://www.gwec.net/fileadmin/images/Publications/GWEC_annual_market_update_2010_-_2nd_ edition_ April_2011.pdf].

Greving, G. & Biermann, W.-D. (2008). Application of the radar cross section RCS for objects on the ground – example of wind turbines, *2008 International Radar Symposium*, IRS, Wroclaw, Poland.

Greving, G., Biermann, W.-D. & Mundt, R. (2009). RCS – numerical, methodological and conceptional aspects for the analysis of radar distorting objects, *11th International Radar Symposium*, IRS, Vilnius, Lithuania.

Greving, G. & Malkomes, M. (2006). On the concept of the radar cross section RCS of distorting objects like wind turbines for the weather radar, *The Fourth European Conference on Radar in Meteorology and Hydrology*, ERAD, Barcelona, Spain, pp. 333–336.

Greving, G. & Malkomes, M. (2008). Weather radar and wind turbines – theoretical and numerical analysis of the shadowing effects and mitigation concepts, *The Fifth European Conference on Radar in Meteorology and Hydrology*, ERAD, Helsinki, Finland.

Haase, G., Johnson, D. & Eriksson, K.-Å. (2010). Analyzing the impact of wind turbines on operational weather radar products, *The Sixth European Conference on Radar in Meteorology and Hydrology*, ERAD, Sibiu, Romania, pp. 276–281.

Hafner, S., Reitter, R. & Seltmann, J. (2004). Developments in the DWD radarnetwork, *The Third European Conference on Radar in Meteorology and Hydrology*, ERAD, Visby, Sweden, pp. 425–427.

Hood, K. T., Torres, S. M. & Palmer, R. D. (2009). Automatic detection of wind turbine clutter using doppler spectral features, *34th Conference on Radar Meteorology*, American Meteorological Society, Williamsburg, VA. Paper P10.1.

Hood, K., Torres, S. & Palmer, R. (2010). Automatic detection of wind turbine clutter for weather radars, *Journal of Atmospheric and Oceanic Technology* 27: 1868–1880.

Høye, G. (2007). Electromagnetic shadow effects behind wind turbines, *FFI Report FFI/RAPPORT-2007/00842*, Norwegian Defence Research Establishment. [Avaiable online at http://rapporter.ffi.no/rapporter/2007/00842.pdf].

Hutchinson, G. & Miles, R. (2008). The protection of weather radar networks. the UK experience, *The Fifth European Conference on Radar in Meteorology and Hydrology*, ERAD, Helsinki, Finland.

Isom, B. M., Palmer, R. D., Secrest, G. S., Rhoton, R. D., L., D. S. T., Allmon, Reed, J., Crum, T. & Vogt, R. (2009). Detailed observations of wind turbine clutter with scanning weather radars, *Journal of Atmospheric and Oceanic Technology* 26: 894–910.

Jago, P. & Taylor, N. (2002). Wind turbines and aviation interests — European experience and practice, *Department of Trade and Industry report ETSU W/14/00624/REP*, STASYS Ltd.

Keeler, R. J. & Serafin, R. J. (2008). Meteorological radar, *in* M. Skolnik (ed.), *Radar Handbook*, 3 edn, McGraw-Hill.

Kent, B. M., Hill, K. C., Buterbaugh, A., Zelinski, G., Hawley, R., Cravens, L., Tri-Van, Vogel, C. & Coveyou, T. (2008). Dynamic radar cross section and radar Doppler measurements of commercial general electric windmill power turbines part 1: Predicted and measured radar signatures, *IEEE Antennas Propagation Magazine* 50: 211–219.

Kong, F., Zhang, Y., Palmer, R. & Bai, Y. (2011). Wind turbine radar signature characterization by laboratory measurements, *Radar Conference (RADAR)*, IEEE.

Lemmon, J. J., Caroll, J. E., Sanders, F. H. & Turner, D. (2008). Assessment of the effects of wind turbines on air traffic control radars, *NTIA Technical Report TR-08-454*, US Department of Commerse, National Telecommunications & Information Administration.

Manwell, J., McGowan, J. & Rogers, A. (2009). *Wind Energy Explained: Theory, Design and Application*, 2 edn, John Wiley & Sons, Ltd.

Michelson, D. B., Andersson, T., Koistinen, J., Collier, C. G., Riedl, J., Szturc, J., Gjertsen, U., Nielsen, A. & Overgaard, S. (2000). BALTEX radar data centre products and their methodologies, *RMK 90*, Swedish Meteorological and Hydrological Institute.

Nai, F., Palmer, R. & Torres, S. (2011). Wind turbine clutter mitigation using range-Doppler domain signal processing method, *27th Conf. on Interactive Information and Processing Systems*, American Meteorological Society, Seattle, WA. Paper 9.4.

Ohs, R. R., Skidmore, G. J. & Bedrosian, G. (2010). Modeling the effects of wind turbines on radar returns, *The 2010 Military Communications Conference*, MILCOM, San Jose, CA, pp. 272–276.

OPERA (2010). Statement of the OPERA group on the cohabitation between weather radars and wind turbines, [Available online at http://www.knmi.nl/opera/opera3/OPERA_2010_14_Statement_on_weather_radars_and_wind_turbines.pdf].

Ousbäck, J.-O. (1999). Försvaret och vindkraften. Huvudstudie radar, *Slutrapport 99-2936/L*, Försvarets forskningsanstalt (FOA). In Swedish.

Poupart, G. J. (2003). Wind farms impact on radar aviation interests, *Final Report FES W/14/00614/00/REP, DTI PUB URN 03/1294*, QinetiQ.

Price, T. J. (2005). James Blyth—Britains first modern wind power pioneer, *Wind Engineering* 29(3): 191–200.

RABC & CanWEA (2007). Technical information and guidelines of the assessment of the potential impact of wind turbines on radiocommunication, radar and seismoacoustic systems, *Technical report*, Radio Advisory Board and Canadian Wind Energy Association.

Rashid, L. & Brown, A. (2010). Partial treatment of wind turbine blades with radar absorbing materials (RAM) for RCS reduction, *Proceedings of the Fourth European Conference on Antennas and Propagation*, EuCAP, Barcelona, Spain.

Seltmann, J. & Lang, P. (2009). Impact of wind turbines on radar measurements and tracking processes. Internal study commisioned by TI.

Sengupta, D. L. (1984). Electromagnetic interference effects of wind turbines, *The Working Committee on EMI*, International Energy Association, Copenhagen, Denmark.

Sengupta, D. L. & Senior, T. B. A. (1979). Electromagnetic interference to television reception caused by horizontal axis windmills, *Proceedings of the IEEE* 67: 1133–1142.

Senior, T. B. L., Sengupta, D. L. & Ferris, J. E. (1977). TV and FM interference by windmills, *Technical Report E(11-1)-2846*, Energy Research and Development Administration.

Shepard, D. G. (1990). Historical development of the windmill, *Contractor Report 4337 DOE/NASA/5266-1*, NASA.

Skolnik, M. (2008). An introduction and overview of radar, *in* M. Skolnik (ed.), *Radar Handbook*, 3 edn, McGraw-Hill.

Sparven Consulting (2001). Wind turbines and radar: Operational experience and mitigation measures, *Technical report*, Sparven Consulting.

Summers, E. (2001). The operational effects of wind farm developments on ATC procedures for Glasgow Prestwick international airport, *Technical report*, Glasgow Prestwick International Airport.

Toth, M., Jones, E., Pittman, D. & Solomon, D. (2011). DOW radar observations of wind farms, *Bulletin of the American Meteorological Society* 92(11): 987–995.

Tristant, P. (2006a). Impact of wind turbines on weather radars band, *Report to WMO, Commission for Basic Systems Steering Group on Radio Frequency Coordination CBS/SG-RFC 2006/Doc. 3.1(6)*, Météo France. [Available online at http://www.wmo.int/ pages/prog/www/TEM/SG-RFC06/Wind turbine vs weather radars.doc].

Tristant, P. (2006b). Radio frequency threats on meteorological radar operations, *The Fourth European Conference on Radar in Meteorology and Hydrology*, ERAD, Barcelona, Spain.

Vogt, R. J., Crum, T. D., Greenwood, W., Ciardi, E. J. & Guenther, R. G. (2011). New criteria for evaluating wind turbine impacts on NEXRAD radars, *WINDPOWER 2011*, American Wind Energy Association Conference and Exhibition, Anaheim, CA.

Vogt, R. J., Crum, T. D., Reed, J. R., Ray, C. A., Chrisman, J. N., Palmer, R. D., Isom, B., Snow, J. T., Burgess, D. W. & Paese, M. S. (2007a). Weather radars and wind farms — working together for mutual benefit, *WINDPOWER 2007*, American Wind Energy Association Conference and Exhibition, Los Angeles, CA.

Vogt, R. J., Crum, T. D., Sandifer, J. B., Ciardi, E. J. & Guenther, R. G. (2009). A way forward wind farm — weather radar coexistence, *WINDPOWER 2009*, American Wind Energy Association Conference and Exhibition, Seattle, WA.

Vogt, R. J., Reed, J., Crum, T., Snow, J. T., Palmer, R., Isom, B. & Burgess, D. W. (2007b). Impacts of wind farms on WSR-88D operations and policy considerations, *23rd International Conference on Interactive Information and Processing Systems for Meteorology, Oceanography, and Hydrology*, American Meteorological Society, San Antonio, TX. Paper 5B.7.

Webster, D. M. (2005a). The effects of wind turbine farms on air defence radars, *Technical Report AWC/WAD/72/652/TRIALS*, Air Warfare Centre, Waddington, United Kingdom.

Webster, D. M. (2005b). The effects of wind turbine farms on ATC radar, *Technical Report AWC/WAD/72/665/TRIALS*, Air Warfare Centre, Waddington, United Kingdom.

WMO (2010). Commission for instruments and methods of observation, *Fifteenth session WMO-No.1046*, World Meteorological Organization. [Available online at http://www.wmo.int/pages/prog/www/CIMO/CIMO15-WMO1064/1064_en.pdf].

Woodcroft, B. (1851). *The Pneumatics of Hero of Alexandria from the original Greek*, Taylor Walton and Maberly, London. [Available online at http://www.history.rochester.edu/steam/hero].

Wright, D. T. & Eng, C. (1992). Effects of wind turbines on UHF television reception, *Fifteenth session BBC RD 1992/7*, BBC Research Department.

Zhang, Y., Huston, A., Palmer, R. D., Albertson, R., Kong, F. & Wang, S. (2011). Using scaled models for wind turbine EM scattering characterization: Techniques and experiments., *IEEE T. Instrumentation and Measurement* 60: 1298–1306.

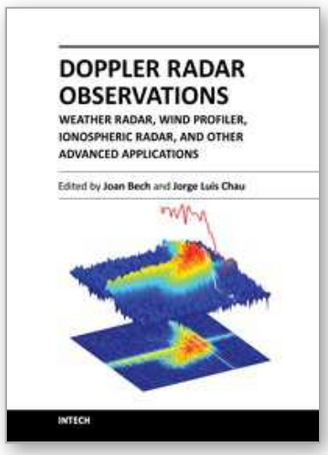

Doppler Radar Observations - Weather Radar, Wind Profiler, Ionospheric Radar, and Other Advanced Applications

Edited by Dr. Joan Bech

ISBN 978-953-51-0496-4
Hard cover, 470 pages
Publisher InTech
Published online 05, April, 2012
Published in print edition April, 2012

Doppler radar systems have been instrumental to improve our understanding and monitoring capabilities of phenomena taking place in the low, middle, and upper atmosphere. Weather radars, wind profilers, and incoherent and coherent scatter radars implementing Doppler techniques are now used routinely both in research and operational applications by scientists and practitioners. This book brings together a collection of eighteen essays by international leading authors devoted to different applications of ground based Doppler radars. Topics covered include, among others, severe weather surveillance, precipitation estimation and nowcasting, wind and turbulence retrievals, ionospheric radar and volcanological applications of Doppler radar. The book is ideally suited for graduate students looking for an introduction to the field or professionals intending to refresh or update their knowledge on Doppler radar applications.

INTECH
open science | open minds

InTech Europe
University Campus STeP Ri
Slavka Krautzeka 83/A
51000 Rijeka, Croatia
Phone: +385 (51) 770 447
Fax: +385 (51) 686 166
www.intechopen.com

InTech China
Unit 405, Office Block, Hotel Equatorial Shanghai
No.65, Yan An Road (West), Shanghai, 200040, China
中国上海市延安西路65号上海国际贵都大饭店办公楼405单元
Phone: +86-21-62489820
Fax: +86-21-62489821

IntechOpen